Influence of the Low-Pass Filter Order to the Attenuation Deviation at the High Frequencies

Bohumil Brtník
Department of Electrical Engineering
University of Pardubice
Pardubice, Czech Republic
bohumil.brtnik@upce.cz

David Matoušek
Department of Electrical Engineering
University of Pardubice
Pardubice, Czech Republic
david.matousek@upce.cz

***Abstract*—The Sallen-Key low-pass biquad shows a decrease in attenuation at high frequencies because the real operational amplifier has a finite transit frequency. As a result, the course of the actual frequency response deviates from the ideal. Generally, this phenomenon occurs only in even-order filters in both Voltage Mode (VM) and Current Mode (CM) but is no longer observed for odd-order filters. When determining the order of the filter, it is always necessary to round the calculated value upwards, so it is discussed whether it is appropriate to round it up to the nearest odd number. Finally, this method of attenuation decrease correction is compared with the correction using another active element.**

Keywords—low-pass filter, attenuation drop above transit frequency, voltage mode, current mode, higher-order filter

I. INTRODUCTION

The main disadvantage of all types of time-discrete signal processing, whether digital filters or filters with Switched Capacitors (SC) or filters with Switched Currents (SI), is the periodicity of their frequency response. This leads to an overlap of the spectra of signals whose frequency is greater than half the sampling frequency in discrete processing, which is unacceptable. Therefore, a Low-Pass (LP) anti-aliasing filter must be included at the input of the circuits. The output low-pass reconstruction filter then removes high-frequency quantization noise [1].

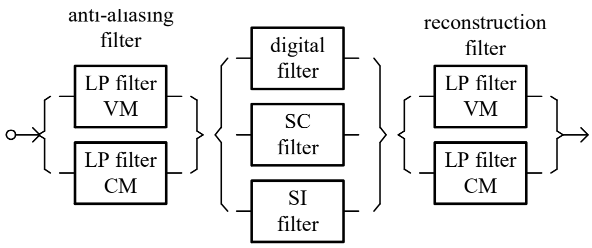

Fig. 1. Anti-aliasing and reconstruction filter for time-discrete signal processing.

When designing a low-pass anti-aliasing filter, the cut-off frequency f_C and the maximum attenuation A_C in the passband are given, as well as the minimum attenuation in the non-passband A_S, which starts from the frequency f_S. The curve corresponds to this and is shown in Fig. 2.

In Fig. 2, the waveforms marked *a* and *c* correspond to the limit cases of the ideal filter. The waveform marked *b* then corresponds to the practical frequency characteristic for the filter with the influence of the transit frequency of the operational amplifier.

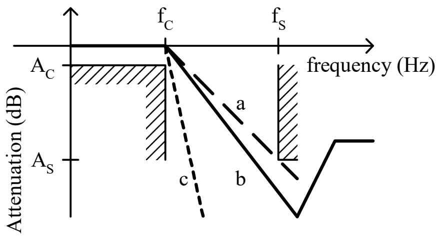

Fig. 2. The course of frequency characteristics of anti-aliasing filter.

From the previously mentioned values A_C, A_S, f_C, and f_S, the anti-aliasing filter order n is calculated by (1).

$$n = \frac{\log\left(\dfrac{10^{\frac{A_C}{10}}-1}{10^{\frac{A_S}{10}}-1}\right)}{2\cdot\log\left(\dfrac{f_C}{f_S}\right)} \tag{1}$$

The calculated filter order must round up to an integer because the number of orders can only be an integer. However, this necessarily leads to the transition from the pass-band to the stop-band always having a greater steepness, i.e., a narrower transition zone than its required width. Rounding down is impossible because the condition of suppressing signals higher than half the sampling frequency (Shannon's sampling theorem) is not accomplished.

Active RC (ARC) filters are generally used to implement anti-aliasing and reconstruction filters. However, low-pass filters of some structures, such as the biquad Sallen-Key structure [1], [2], [3], [4], [5], and some others, show a decrease in attenuation above the transit frequency of the operational amplifier. Then the frequency response of the filter is shown by the course *b* in Fig. 2. The same phenomenon occurs in the stop-band zone at the bandpass of the Huelsmann and Deliyanis structures.

The cause of this phenomenon is that the operational amplifier, after losing its gain *A* above the transit frequency, shows only the output conductivity *g*, which with the dominant conductivity *G* connected to the input node forms the voltage divider according to Fig. 3 (capacitors act as a short circuits for high frequencies). The effect of conductivity *G* connected in parallel with the output conductivity *g* can be neglected. This in turn leads to stagnation or even a decrease in the attenuation according to Fig. 3.

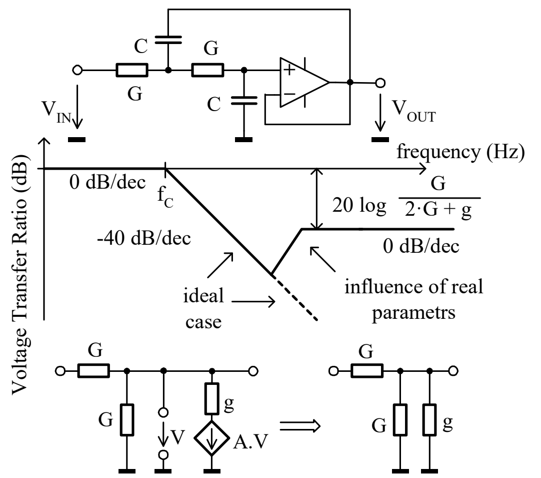

Fig. 3. Biquad low-pass of the Sallen-Key structure on the top, its frequency response in the middle and its model in high frequencies below.

Therefore, the magnitude of the voltage transfer ratio at the highest frequencies must be not equal to zero in this case:

$$F_{\inf} = \lim_{\omega \to \infty} \frac{V_{OUT}}{V_{IN}} = \frac{-(-G)}{2 \cdot G + g} = \frac{G}{2 \cdot G + g} \neq 0 \qquad (2)$$

where: F_{inf} is the magnitude of the voltage transfer ratio close to infinity frequency, V_{IN}, V_{OUT} are the input and output voltages, g is the series output conductance of the operational amplifier, G is the conductance of a working resistor in the filter.

The theoretical course can be easily verified by simulation with the MicroCap-12 program, where $C = 10$nF and $R = 1$kOhm, operational amplifier OP77 with $R_{OUT} = 75$Ohm and $GBW = 600$kHz were used. The simulation result is shown in Fig. 4.

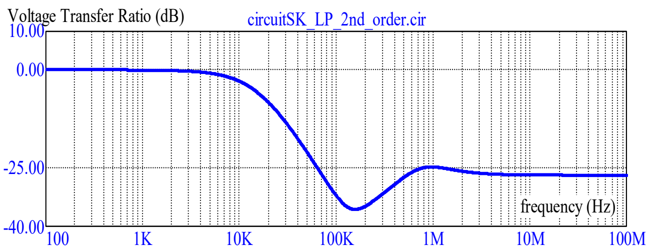

Fig. 4. Result of simulation of the second-order low-pass Sallen-Key filter (generated in MicroCap-12).

II. Analysis of the Course of Low-Pass Characteristics in Voltage and Current Mode

A decrease in attenuation in the high-frequency range also occurs with the low-pass filter in current mode [2], [3], [4], [6], realized by the associated transformation from the circuit in voltage mode (Fig. 5 on the left), if it is active element used current conveyor (Fig. 5 on the right).

The original circuit from the right side of Fig. 5 is redrawn in Fig. 6. Component F1 is Current Controlled Current Source (CCCS) with $K = 1$, but input resistance can't be zero, therefore it will be the value approaching zero, e.g., $r = R3 = 0.1$Ohm. If input resistance is equal to zero, then the branch with capacitor C_2 will be initialized by the zero voltage in the node #2 and therefore described effect doesn't appear.

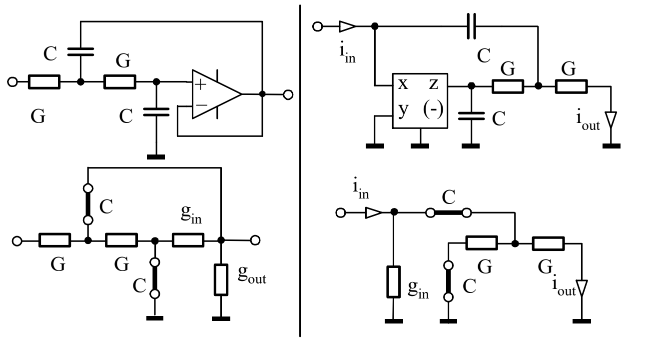

Fig. 5. Low-pass Sallen-Key biquad in voltage mode (on the left) and current mode with conveyor (on the right) with simplified circuits diagram for high frequencies.

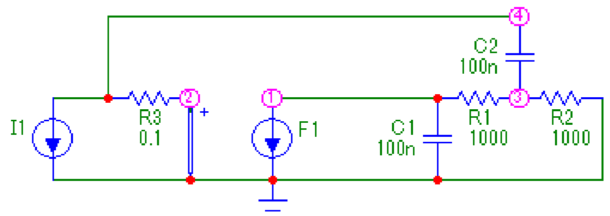

Fig. 6. Schematic diagram of original circuit drawn in MicroCap-12.

From simulated results (see Fig. 7), the difference between maximal and minimal magnitude is 80dB, this value is corresponding to the ratio between input current and the output current (i.e., R_2 between input resistance R_3 of the CCCS).

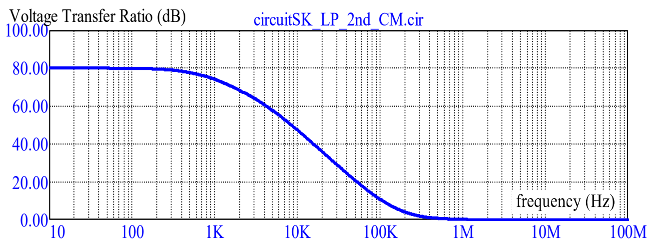

Fig. 7. Result of simulation of the second-order low-pass Sallen-Key filter in current mode (generated in MicroCap-12).

Thus, the higher-order filter composed exclusively of second-order sub-blocks (biquads) will behave similarly in voltage and current modes. Therefore, the frequency response of an even-order filter deviates from the frequency response of an ideal filter when the attenuation does not increase monotonically but stagnates.

However, the third-order filter, whose voltage mode diagram is in Fig. 8, does not have this disadvantage. The cause is the capacitor C of the input RC cell, which behaves like a short circuit at high frequencies, the voltage Vi is zero, so at high frequencies, the rest of the circuit is not excited in both voltage and current mode. The output voltage of the filter is zero and then filter attenuation increases monotonically.

The frequency response of the third-order filter is therefore close to the frequency response of an ideal filter. This theoretical premise can be easily verified through a simulation with the program MicroCap-12, when the values of elements we choose for the same cut-off frequency as for the previous 2nd order filter, i.e., for 10kHz. The result of the simulation shows in Fig. 9.

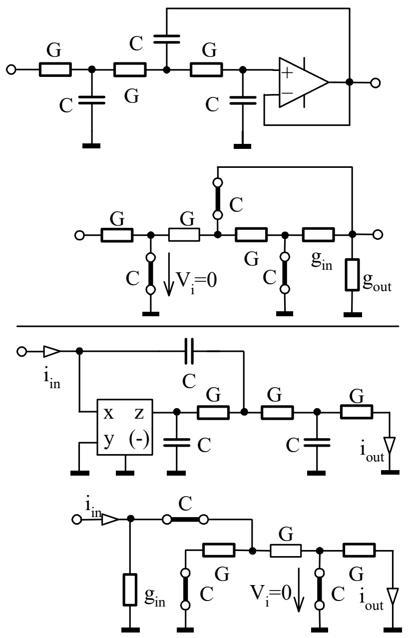

Fig. 8. Low-pass Sallen-Key third-order filter in voltage mode (on the top) and current mode with conveyor (on the bottom) with simplified circuit diagrams for high frequencies.

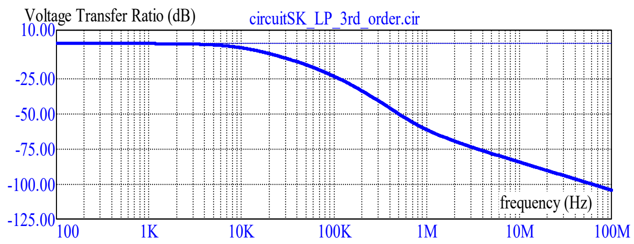

Fig. 9. Result of simulation of the third-order low-pass Sallen-Key filter in voltage mode (generated in MicroCap-12).

This phenomenon also occurs with the low-pass filter in current mode, realized by the associated transformation from the circuit in voltage mode [7], [8], [9], [10], when a current conveyor works as the active element (Fig. 8 below). A higher-order filter that contains at least one third-order block (Fig. 10) will behave the same. Therefore, the frequency response of a generally odd-order filter is close to the frequency response of an ideal filter.

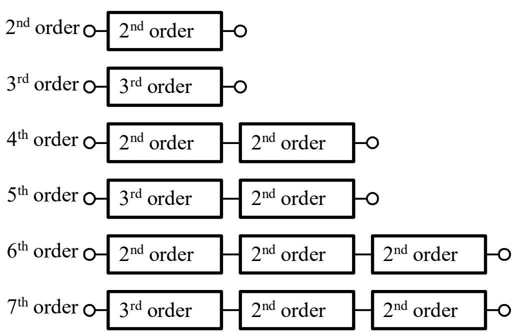

Fig. 10. Cascade ordering of partial filters in odd-order filters.

To Fig. 10, we can add the information that the 6th order filter cannot implement using two cascaded 3rd order filters. The 3rd order filter has one real pole of the frequency response. If we use two such filters in a cascade, these real poles would be identical.

If the calculation (1) after rounding gets an even number (an even-order filter), but if the next higher odd-order we use for the construction of higher-order filters instead of even ones, the characteristics of the high-frequency filter will approach the ideal course.

III. Discussion of a Solution Based on Adding Another Active Element to the Filter Feedback

Another well-known possibility of solving the problem of degradation of the attenuation of the filter at high frequencies is to connect another operational amplifier in voltage mode [6] or conveyor in current mode [11], [12] of the filter, according to Fig. 11.

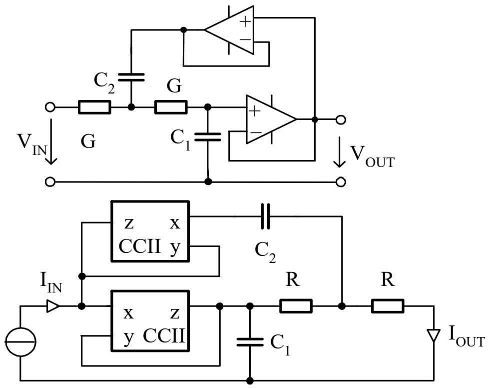

Fig. 10. Correction of the attenuation decrease by another active element in the feedback in voltage mode (on the top) and current mode (on the bottom).

However, the transmission T of such a circuit with two active elements differs from the transmission of the original circuit with a single active element, as can be seen (at first glance) from a comparison of the Mason-Coates graphs (MC-graphs) of these circuits shown for voltage mode in Fig. 12.

According to Fig. 12 on the left, the transmission T for two active elements is (3).

$$T = \frac{G^2 \cdot A}{(sC_2 + 2 \cdot G) \cdot (sC_1 + G) - G^2 - G \cdot A^2 \cdot sC_2} \tag{3}$$

Meanwhile, for a circuit with a single active element in a straight branch, the MC-graph form Fig. 12 on the right generates a result transmission (4).

$$T = \frac{G^2 \cdot A}{(sC_2 + 2 \cdot G) \cdot (sC_1 + G) - G^2 - G \cdot A \cdot sC_2} \tag{4}$$

The difference between the two transmissions is more clearly reflected in the frequency dependence of the gain of the operational amplifier in the open feedback loop, which is given by the relation (5) for the two refractive frequencies of this characteristic ω_T (transit frequency, about 1MHz), ω_{OL} (−3dB frequency of the open-loop response, about 10Hz).

$$\frac{V_{OUT}}{V_{IN}} = \frac{A \cdot \omega_T}{\omega_T + sA} \cdot \frac{\omega_{OL}}{\omega_{OL} + s} \tag{5}$$

The transmission determines (6) for a circuit with two active elements and (7) for a circuit with a single active element.

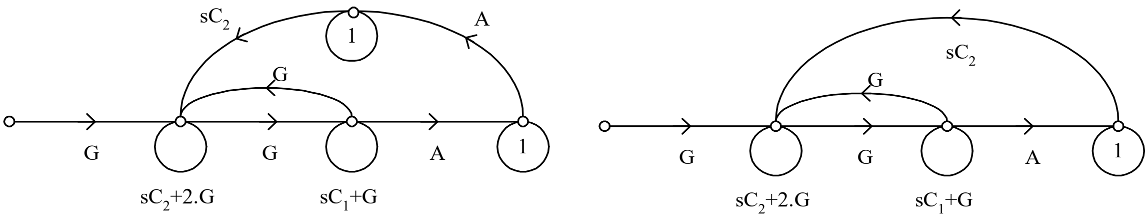

Fig. 11. MC circuit graph with two active elements (on the left) and MC circuit graph with single active element (on the right).

$$T = \frac{G^2 \cdot \dfrac{A \cdot \omega_T}{\omega_T + sA} \cdot \dfrac{\omega_{OL}}{\omega_{OL} + s}}{(sC_2 + 2 \cdot G) \cdot (sC_1 + G) - G^2 - G \cdot \dfrac{A \cdot \omega_T}{\omega_T + sA} \cdot \dfrac{\omega_{OL}}{\omega_{OL} + s} \cdot \dfrac{A.\omega_T}{\omega_T + sA} . \dfrac{\omega_{OL}}{\omega_{OL} + s} \cdot sC_2} \tag{6}$$

$$T = \frac{G^2 \cdot \dfrac{A \cdot \omega_T}{\omega_T + sA} \cdot \dfrac{\omega_{OL}}{\omega_{OL} + s}}{(sC_2 + 2 \cdot G) \cdot (sC_1 + G) - G^2 - G \cdot \dfrac{A \cdot \omega_T}{\omega_T + sA} \cdot \dfrac{\omega_{OL}}{\omega_{OL} + s} \cdot sC_2} \tag{7}$$

CONCLUSION

In conclusion, one of the ways to eliminate the decrease in attenuation of the low-pass filter at high frequencies is to implement a filter composed only of blocks of odd orders.

However, this modification increases the steepness of the frequency characteristic between the pass-band and the stop-band, according to Fig. 2 variant c. The course of the frequency characteristic is thus much stricter than required, but quite analogously, as it is less strict with the necessary round of the calculated filter order upwards.

Thus, we can say that by choosing an odd order, we always get closer to the ideal course of the frequency response at the cost of increasing the filter order by one. This consequence is not a problem. Thus, when we determine the filter order, we always round result up, i.e., the resulting order is always higher than the calculating value. However, the frequency response of the transmission doesn't change with the comparison with the use of another active element in the feedback.

REFERENCES

[1] Ch. Toumazou, F. J. Lidgey, and D. G. Haigh, Analogue IC design the current-mode approach, 1st ed. London: Peter Peregrinus, 1990, pp. 446-447.

[2] D. Biolek, Solving electronic circuits, 1st ed., Prague: BEN, 2004.

[3] S. Winder, Analogue and digital filter design, 2nd ed., Oxford: Elsevier, 2002, pp. 133-135.

[4] L. Thede, Practical analog and digital filter design, 1st ed., London: Artech House, Inc., 2004, pp. 87-95.

[5] J. Puncochar, “Low-pass filters Sallen and Key with real operational amplifiers,” Elektrorevue 10, 2005, pp. 1-13.

[6] P. Martinek, P. Boreš, and J. Hospodka, The electric filters, 1st ed., Prague: CTU Publisher, 2003, pp. 98-101.

[7] Ch. Toumazou, J. B. Hughes, and N.C. Battersby, Switched current an analogue technique, 1st ed., London: Peter Peregrinus Ltd, 1993.

[8] T. Dostál, Theory of electric circuits, 1st ed., Brno: BUT, 2004, pp. 172-196.

[9] J. Bicak, M. Leipert, and M. Vlcek, A linear circuits an systems, 1st ed. Prague: CTU publisher, 2007.

[10] G. W. Roberts and A. S. Sedra, “All current-mode frequency selective circuits,” Electron. Lett., 25(12), 1989, pp. 759-761.

[11] B. Brtník and D. Matoušek, “Correction of the attenuation of the low-pass biquad in the current mode based on prototype in voltage mode,” Acta Electrotechnica et Informatica, 2(16), 2016, pp.8-11.

[12] B. Brtník and D. Matoušek, “The flow graph usage for the attenuation correction of the low-pass Sallen-Key biquad in the current mode,” in Proceedings 2016 International Conference on Applied Electronics, Plzeň, Czech Republic, pp.39-42, September 2016.